PRAMANA — journal of physics
© Indian Academy of Sciences
Vol. 75, No. 1
July 2010
pp. 3–12

Gamma and electron spectroscopy of transfermium isotopes at Dubna: Results and plans

A YEREMIN[1,*], O MALYSHEV[1], A POPEKO[1], A LOPEZ-MARTENS[2], K HAUSCHILD[2], O DORVAUX[3], S SARO[4], D PANTELICA[5] and S MULLIN[6]
[1]Flerov Laboratory of Nuclear Reactions, Joint Institute for Nuclear Research, Joliot Curie Str. 6, 141980 Dubna, Russia
[2]CSNSM, IN2P3-CNRS, Orsay Campus, F-91405 Orsay, France
[3]IPHC, IN2P3-CNRS, F-67037 Strasbourg, France
[4]Comenius University, SK84215 Bratislava, Slovakia
[5]Inst. for Physics and Nuclear Engineering, Bucharest Magurele, P.O. Box MG6, Romania
[6]iThemba Labs, South Africa
*Corresponding author. E-mail: eremin@jinr.ru

Abstract. Detailed spectroscopic information of excited nuclear states in deformed transfermium nuclei is scarce. Most of the information available today has been obtained from investigations of fine-structure α-decay. Although α decay gives access to hindrance factors and lifetimes which are strongly correlated to shell/subshell closures and the presence of isomers, only the combined use of γ and conversion electron spectroscopy allows the precise determination of excitation energy, spin and parity of nuclear levels.

In the years 2004–2009 using the GABRIELA set-up [Hauschild *et al*, *Nucl. Instrum. Methods* **A560**, 388 (2006)] at the focal plane of VASSILISSA separator [Malyshev *et al*, *Nucl. Instrum. Methods* **A440**, 86 (2000); **A516**, 529 (2004)] experiments with the aim of γ and electron spectroscopy of the isotopes from Fm to Lr, formed by complete fusion reactions with accelerated heavy ions were performed. In the following, the preliminary results of decay studies using α–γ and α–β coincidences at the focal plane of the VASSILISSA recoil separator are presented.

Accumulated experience allowed us to perform ion optical calculations and to design the new experimental set-up, which will collect the base and best parameters of the existing separators and complex detector systems used at the focal planes of these installations. In the near future it is planned to study neutron-rich isotopes of the Rf–Sg in the 'hot' fusion reactions with ^{22}Ne incident projectiles and ^{242}Pu, ^{243}Am and ^{248}Cm targets.

Keywords. Recoil separator; heavy ion-induced reactions; properties of nuclei with $220 \leq A$; γ-transitions and level energies.

PACS Nos 23.20.Lv; 23.60.+e; 27.90.+b; 29.30.Kv

1. Introduction

The heaviest elements provide a unique laboratory to study nuclear structure and nuclear dynamics under the influence of large Coulomb forces and large mass (A).

The stability of nuclei beyond the spherical 'doubly magic' ^{208}Pb decreases rapidly until the transfermium region ($Z \geq 100$) where a lowering of the level density of single-particle states for nuclei in the neighbourhood of the deformed doubly magic $^{270}_{108}$Hs reverses this trend locally [1]. However, the position of the spherical doubly magic nucleus beyond ^{208}Pb remains controversial: recent calculations predicting $Z = 114$, 120, or 126 for the next magic proton shell, and $N = 172$ or 184 for neutrons [2–4].

Important information on the structure of super heavy elements (SHE) can come from the study of lighter deformed transfermium ($Z \approx 100$–106) elements. The cross-section for the formation of these nuclei is many orders of magnitude larger than for $Z \geq 110$ so that detailed spectroscopy becomes possible. However, beyond einsteinium ($Z = 99$), detailed spectroscopic data are sparse. One of the methods to populate the nuclei of interest is via heavy-ion fusion evaporation (HI,xn) reactions. In this case, it is the overwhelming background from the predominant fission channel that needs to be addressed. This has been achieved with gas-jet transport systems and in-flight recoil separators. Recently, spectroscopic studies in this mass region have seen intense activity in two distinct directions: (1) prompt in-beam spectroscopy at the target position exploiting the recoil decay tagging (RDT) method and (2) isomeric and/or decay spectroscopy at the focal plane of the recoil separator.

A number of rotational bands have now been observed using both γ-ray and conversion electron (CE) spectroscopy: ^{254}No [5–8], ^{253}No [7,9], ^{252}No [10], ^{250}Fm [11] and ^{251}Md [12]. These results and additional unpublished data have been reviewed in ref. [13].

However, focal plane decay studies using α–γ coincidence measurements have only been reported for a few transfermium nuclei: ^{251}No [14], ^{253}No [13,15], ^{255}Lr [16] and ^{255}Rf [17]. The α–γ coincidence and α–CE coincidence decay spectroscopy of ^{257}No [18] present an interesting development with the re-emergence of gas-jet systems. In these high Z nuclei, internal conversion becomes an extremely important decay mode since it can compete effectively with γ-decay. This makes it essential to perform electron spectroscopy together with γ-spectroscopy and is the motivation behind the project GABRIELA [19,20].

2. Experiment

The joint JINR–IN2P3 (France) project entitled 'Study of nuclear structure and nuclear reaction mechanism of heavy and superheavy elements: Gamma and electron spectroscopy of very heavy nuclei with $Z \geq 104$' started in the year 2004. This project aimed at the nuclear spectroscopy of transfermium elements using high-intensity heavy ion beams from FLNR cyclotron U400, exotic (radioactive) targets and recoil separator VASSILISSA. In the framework of this collaboration, GABRIELA – Gamma Alpha Beta Recoil Investigation with the Electromagnetic Analyser – project was very fruitfully continuing for the last five years using heavy ion beams of FLNR cyclotron U400 and kinematic separator VASSILISSA. Photo of the GABRIELA set-up is presented in figure 1.

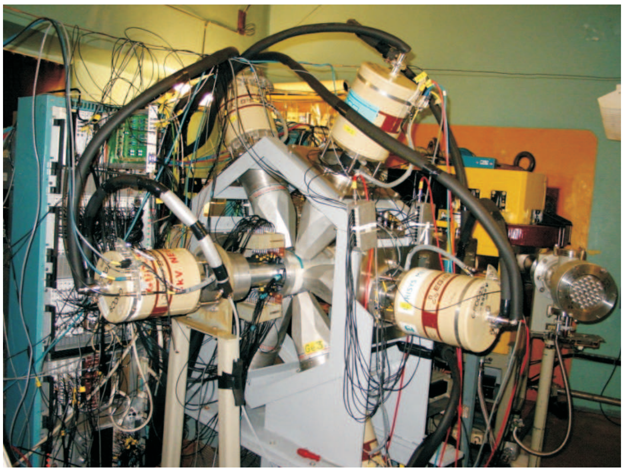

Figure 1. Photo of the detector array GABRIELA at the focal plane of the VASSILISSA separator.

In our set-up, the recoiling products (ER's) were selected by the recoil separator VASSILISSA [21,22]. An additional dipole magnet installed behind the separator on the other side of a 2 m concrete wall provided 8° deflection for the ER's and gave an additional background suppression by a factor of 10–50 for the scattered beam projectiles.

The detector system consisting of two (start and stop) time-of-flight detectors and an array of silicon detectors was installed at the separator focal plane behind the dipole magnet. Having passed the time-of-flight detectors, the recoil nuclei were implanted into the 16-strip Si stop detector. The active area of the silicon strip detector was 60×60 mm^2. Each strip is position sensitive in the vertical direction with a resolution of 0.3–0.5 mm between α-decays of the α-decay chain. In the backward direction from the focal plane stop detector, four electron detectors were placed, which covered 30% of the hemisphere. Each electron detector was 50×50 mm^2 in size and was divided into four strips. In addition, the focal plane detector was surrounded by seven Ge detectors. One Ge detector was placed behind the focal plane strip detector (distance between Si and Ge crystals was about 35 mm), the other six detectors were placed in a ring around the detector chamber looking to the front surface of the focal plane detector (see figure 1).

The detectors of the array were checked with different α-, β- and γ-sources. Also to test the detector system together with electronic and data acquisition systems, a number of experiments were performed. Within this program the complete fusion reactions ^{48}Ca + ^{164}Dy $\rightarrow$ ^{212}Rn*, ^{40}Ar + ^{174}Yb $\rightarrow$ ^{214}Ra* and ^{40}Ar + ^{181}Ta $\rightarrow$ ^{221}Pa* at the excitation energies of compound nuclei corresponding to the de-excitation channels with the evaporation of 4–5 neutrons were studied.

The average energy resolution of 20 keV (FWHM) for α's of the ^{241}Am source was obtained for the silicon strip focal plane detector. An average energy resolution of about 8–10 keV (FWHM) for 322 keV electrons of the ^{133}Ba source was measured for side β-detectors. The Ge detectors had a resolution of about 2.5 keV for the 1408 keV line of the ^{152}Eu γ-source.

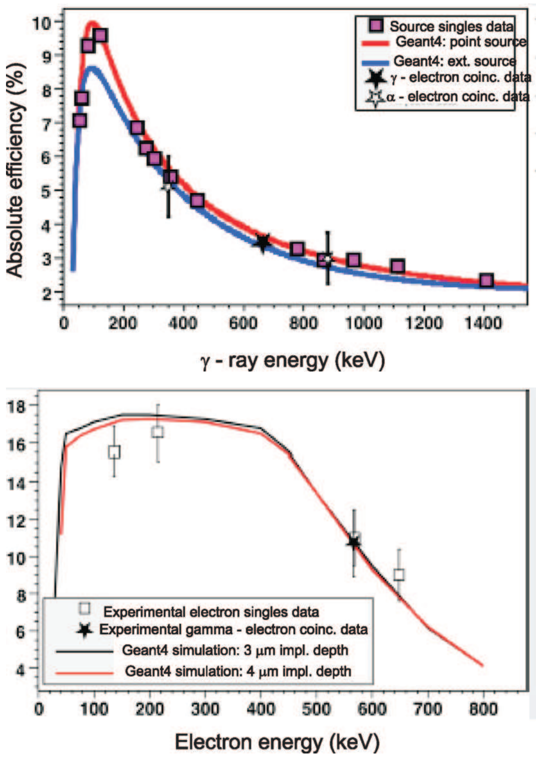

Figure 2. The absolute detection efficiency for 7-Ge (top panel) and 4-electron detectors (bottom panel), measured using calibration sources and decays from the test reactions.

The detection efficiency for α-particles emitted by implanted recoil nuclei into the focal plane strip detector was $\approx$50%. The absolute detection efficiency for Ge and β-detectors was measured using calibration sources and the test reaction ^{164}Dy(^{48}Ca,5n)^{207}Rn [20,23] (see figure 2).

Five full scale experimental campaigns were performed using high-intensity accelerated beams of ^{48}Ca, ^{22}Ne, ^{40}Ar and VASSILISSA separator. Combined detector set-up consisted of seven Ge detectors for registration of X-ray and γ-quanta, emitted from investigated nuclei, as well as a large number of silicon strip detectors for registration of γ- and β-radiation in the geometry close to the 4π. ^{197}Au, ^{181}Ta, ^{206,207,208}Pb, ^{182,184}W, ^{238}U targets were used in the experiments. A large amount of experimental data for the radioactive decay of ^{216,217}Th, ^{217}Pa, ^{218,223,225}U, ^{253,254,255}No, ^{255}Lr isotopes and their daughter products – isotopes of ^{219}Ac, ^{215}Ra, ^{221}Pa, ^{251}Md, ^{249,250,251}Fm [23–27] were obtained in the experiments. Due to the high registration efficiency for γ-quanta and electrons, emitted from the investigated nuclei, with the help of α–γ and α–γ–β correlations, new low-energy transitions for ^{249,251}Fm and ^{216}Th nuclei were discovered. New data for isomeric states concerning the occupation of low-lying single-particle levels at the ^{218}U, ^{253,255}No, ^{255}Lr, ^{223,225}U and ^{217}Pa isotopes were obtained.

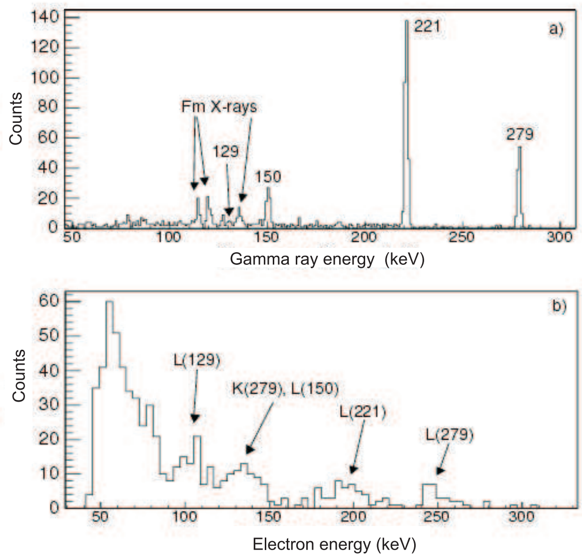

Figure 3. Energy spectrum of γ-rays (**a**) and conversion electrons (**b**) de-exciting levels in ^{249}Fm.

In the case of the heavy evaporation residues, their implantation in the position-sensitive detector is followed mainly by α-decay. In prompt and delayed coincidences with the characteristic α-emission of both mother and daughter nuclei, γ-quanta as well as conversion electrons were detected in GABRIELA.

Excited states in ^{249}Fm were populated in the α-decay of ^{253}No, which was produced in the reaction ^{207}Pb(^{48}Ca,$2n$)^{253}No [23,26]. The spectra of γ-rays and electrons emitted by the excited ^{249}Fm nucleus are shown in figure 3. It reveals the presence of three main γ-transitions at 150, 221 and 279 keV. The equivalent conversion electron spectrum in figure 3 clearly shows the K, L conversion lines of the 279 keV transition as well as the L conversion lines of the 221 keV transition. The K line of this transition is masked by a large structure at 50–70 keV. There are possible signs of L conversion of the 150 keV and of the weak 129 keV γ-line (visible to the left of the last Fm K X-ray group in figure 3).

A search for isomeric decays following the implantation of recoils was performed using the same for the reaction ^{207}Pb(^{48}Ca,$2n$)^{253}No (mainly obtained at the last campaign) [23,27]. Figures 4a and 4b present the logarithm of the time between recoil implantation and subsequent isomeric decay as a function of γ-ray energy and conversion electron energy respectively. The boxes highlight the decays from an isomeric state. The corresponding projections of γ-rays and conversion electrons detected between 8 and 128 μs after a recoil implantation are shown in figures 4c and 4d, respectively. In figure 4c one can clearly see nobelium K X-rays. The difference in energy between the two large conversion electron peaks in figure 4d is consistent with the difference between the L- and MN binding energies in nobelium and corresponds to a transition of 167 keV, also seen in the γ-ray spectrum. The M2 nature of the transition has been deduced from the measured conversion coefficients and a comparison of the intensity of the 167 keV line with the K X-rays. Since

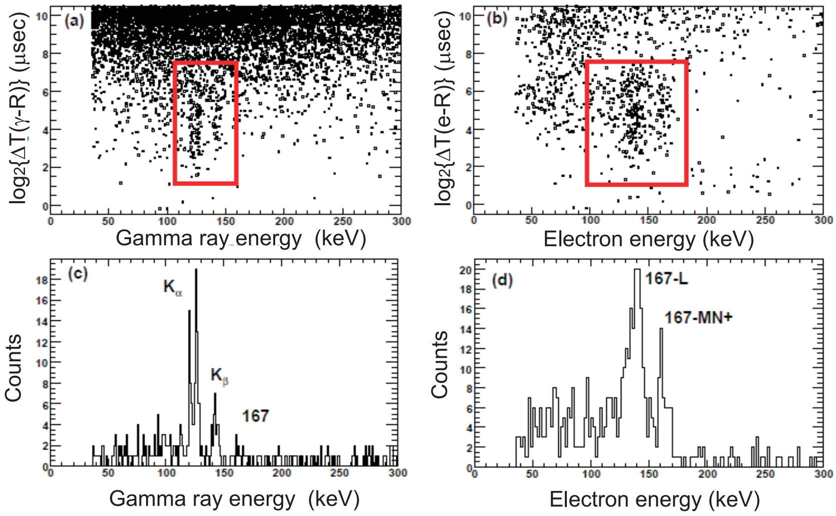

Figure 4. Energy spectra of (**a**) γ-rays and (**b**) conversion electrons as a function of $\log_2(\Delta T)$, where ΔT is the time difference between the detection of recoils and γ-rays or electrons and the corresponding projections onto the energy axis for (**c**) γ-rays and (**d**) conversion electrons observed within 8–128 μs of a recoil implantation. Energies are in keV.

the ground state of ^{253}No has been assigned $9/2^-[734]$ (see [23], we can assign the configuration of this isomer as $5/2^+[622]$). The measured half-life of $t_{1/2} = 31.1(2.1)$ μs is in agreement with that measured by Bemis *et al* [28], but not with recent data measured at SHIP [29].

For ^{255}No, it was observed that many α-decays are followed by delayed γ and electron emissions. Figure 5 shows the time difference ΔT between the α-emission of the evaporation residues implanted in the focal plane detector and the detection of electrons. The time difference is represented in a convenient time-scale, $\ln(\Delta T)/\ln(2)$, inspired by the work of Bartsch *et al* [30] and Schmidt [31].

The delayed peak in figure 5 is correlated to the ^{255}No α group and is due to the presence of an isomeric state in ^{251}Fm. The existence of an isomeric state had been reported in 1971 by Dittmer *et al* [32] but never confirmed in the literature. The half-life was measured to be 26.8(15) μs. From the delayed γ- and β-energy spectra, it was found that this isomeric level de-excites mainly by the emission of a highly converted M2 198 keV transition, which explains the observed lifetime.

The analysis of these data as well as the data collected on ^{253}No in the last campaign is still in progress. It should be mentioned that before the 2009 campaign the focal plane detector and its electronics have been modified and successfully tested for the first time during the experiment. The detector is now a 48×48-strip DSSD. The quality of the detector is very good and a total resolution of 17 keV was obtained (at room temperature). The back face of the detector was equipped with 3 pre-amplification ranges, which allows it to be sensitive to low-energy conversion electrons (0–2 MeV), alpha's (0–20 MeV) and fission fragments (0–200 MeV). In the future, we hope to equip both faces of the detector with such pre-amplifiers

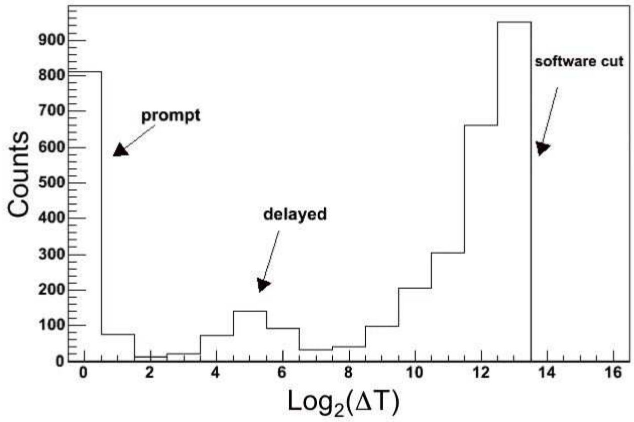

Figure 5. Distribution of time difference (in $\log_2(\mu s)$ scale) between α emission and subsequent β emission in the reaction ^{48}Ca on ^{208}Pb. The prompt peak also contains low-energy escape α's from the main ^{254}No channel and its decay chain.

so that low-energy electrons may be properly position correlated to α-particles or evaporation residues. The transmission of VASSILISSA has also been improved.

3. Modernization of the VASSILISSA separator

The ion optical scheme of the present separator VASSILISSA is Q-Q-Q-E-E-E-Q-Q-Q-D, where Q stands for quadrupole lens, E for electrostatic dipole and D for dipole magnet. In this so-called energy filter, separation of the background products is mainly based on the difference in $E_{\text{ion}}/Q_{\text{ion}}$ ratio where E_{ion} stands for energy of recoil nucleus or reaction product and Q_{ion} for ionic charge respectively. The present set-up is limited in electric rigidity of recoil nuclei by 2 MV (it means that nuclei with energy E_{ion} + 40 MeV and charge state Q_{ion} - 20+ could be transported through the separator). VASSILISSA separator is used in the experiments with a wide range of target–projectile combinations leading to isotopes of transfermium elements – from ^{22}Ne + ^{238}U $\rightarrow$ ^{260}No* to ^{48}Ca + ^{208}Pb $\rightarrow$ ^{256}No*, and provides transmission efficiency for ER's formed in this reaction from 2 to 30% respectively with acceptable factors of the suppression of unwanted products.

The project of the modernization of VASSILISSA set-up has two purposes: to increase transmission efficiency for very asymmetric combinations like ^{22}Ne + ^{238}U or ^{16}O + ^{244}Pu by factors of 2–5 and to extend the region of reactions to be investigated up to symmetric combinations like ^{136}Xe + ^{136}Xe, for which ER's have electric rigidity about 10 MV. It is planned to replace the central separator part, consisting of three electrostatic deflectors, by a combination of two electrostatic deflectors and two dipole magnets creating velocity filter instead of energy filter. This installation will allow one to strongly increase the region of the reactions to be studied upto the extreme case of ^{136}Xe + ^{136}Xe reaction. The ion optical calculations show that the increase of the aperture of the central separator part together with optimization of the ion optical parameters of focussing elements (quadrupole

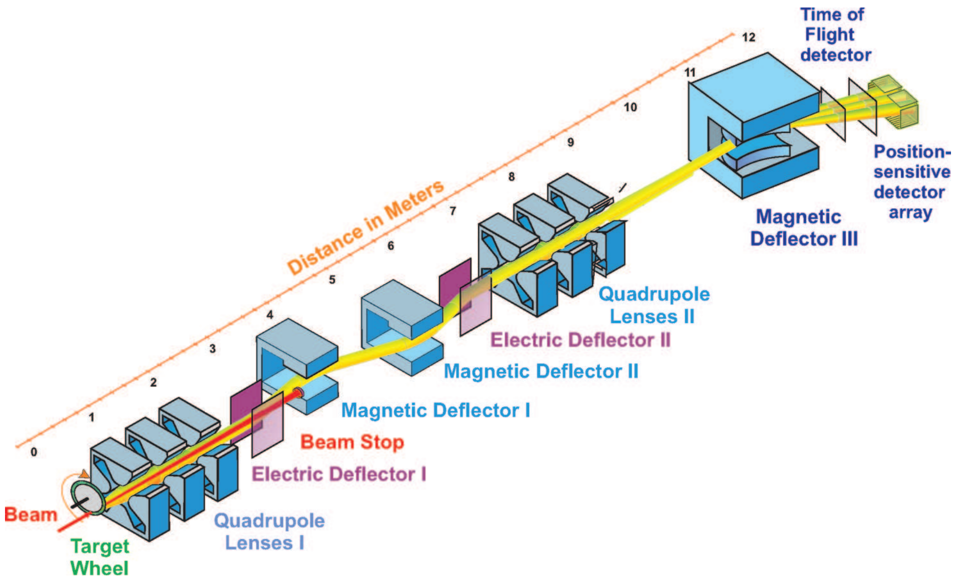

Figure 6. Lay-out of the modernized VASSILISSA separator.

lenses) will allow to increase transmission of slow ER's from asymmetric combinations by factor of at least 3. For this purpose, plates of the electrostatic deflectors are designed to be movable, and it will be possible to change the distance between plates (aperture) to be optimum for the reaction asymmetry.

The principal component of the modernized separator is a system consisting of two combinations of electrostatic and magnetic dipoles, which accomplish spatial filtering of recoil nuclei, multinucleon transfer reaction products and beam particles dispersing them in their velocity and magnetic rigidity. The input focussing system consists of a triplet of magnetic quadrupoles. The triplet is located just behind the target and focusses the evaporation residues emerging from the target forming a quasiparallel beam. The ER's will be deflected in the electric field by an angle of 8° whereas the full energy beam trajectory is practically not affected. Dipole magnets will bend ER's by an angle of 22° each. Maximum dispersion for ER's is reached at the middle point between dipole magnets. The beam is dumped inside the first dipole magnet. After the dispersing system a triplet of magnetic quadrupoles is used, which serves for collecting ER's onto the focal plane detector. Post-separation dipole magnet installed behind the separator and before focal plane detector will provide an 8° deflection for the ER's and will give an additional background suppression for the scattered beam projectiles. Therefore, the modernized separator will be of Q-Q-Q-E-D-D-E-Q-Q-Q-D type and will operate in vacuum mode. It will be 12 m long (see figure 6).

At present in VASSILISSA set-up, the measured transmission for asymmetric, hot fusion reactions using actinide targets is a few per cent only. The reason is the wide solid angle covered by the relatively slow reaction products due to recoil effects from the emitted neutrons ($n \geq 3$) and scattering in the target. For hot fusion reactions, the modernized separator will have an increased acceptance compared

Table 1. Calculated transmission efficiency for modernized separator.

Reaction	$E_{1/2}$ (MeV)	Target thickness (mg/cm^2)	Transmission
$^{22}Ne(^{238}U,5n)^{255}No$	115	U_3O_8 – 0.2	0.09 (now–0.02)
$^{22}Ne(^{238}U,5n)^{255}No$	115	Met – 0.2	0.12
$^{22}Ne(^{197}Au,5n)^{214}Ac$	110	Met – 0.2	0.14
$^{40}Ar(^{181}Ta,4n)^{217}Pa$	182	Met – 0.3	0.28
$^{40}Ar(^{162}Dy,7n)^{195}Po$	198	DyO_2 – 0.3	0.28
$^{48}Ca(^{174}Yb,4n)^{218}Th$	200	YbO_2 – 0.35	0.48
$^{48}Ca(^{208}Pb,2n)^{254}No$	216	Met – 0.4	0.42

Table 2. Estimated counting rates of ER's for modernized separator.

Reaction	Cross-section (nb)	Counting rate per day
$^{238}U(^{26}Mg,5n)^{259}Rf$	1.1	90
$^{242}Pu(^{22}Ne,5n)^{259}Rf$	3.0	110
$^{248}Cm(^{18}O,5n)^{261}Rf$	13	270
$^{244}Pu(^{22}Ne,5n)^{261}Rf$	5.0	180
$^{243}Am(^{22}Ne,5n)^{260}Db$	2.0	70
$^{248}Cm(^{22}Ne,5n)^{265}Sg$	0.3	10
$^{208}Pb(^{54}Cr,1n)^{261}Sg$	0.5	90

to VASSILISSA and comparable suppression factors. A larger aperture will also increase the transmission for the reaction products from 'cold' fusion and due to its higher rigidity, the modernized separator could be used for more symmetric reactions from Ti- to Xe-induced reactions, whereas at VASSILISSA, ^{48}Ca-induced reactions are already close to the limit. All these factors broaden considerably the range of nuclei that can be studied. Calculated transmission efficiencies for ER's from asymmetric target projectile combinations are presented in table 1.

The transmission efficiency for ER's, formed by ^{16,18}O and ^{22}Ne-induced reactions, through the modernized VASSILISSA set-up will be significantly increased. It will allow one to study more neutron-rich isotopes of transfermium elements with counting rates acceptable for the use of γ- and electron spectroscopy (see table 2).

4. Summary

In the future, more neutron-rich No isotopes will be produced using a radioactive ^{238}U target. The ^{255}No and ^{255}Lr experiments will be repeated in order to accumulate more statistics. Also it is planned to investigate the decay properties of neutron-rich ^{259}Rf, formed in the complete fusion reaction $^{242}Pu(^{22}Ne,5n)^{259}Rf$. For the 5n evaporation channel, evaporation residue formation cross-section was measured to be about 5 nb. The transmission efficiency for ER's, formed by ^{22}Ne-induced reactions through the VASSILISSA set-up is about 5%. It results in a counting rate of about 100 Rf ER's per day at a beam intensity of 1 pμA and a target thickness of 200 $\mu g/cm^2$.

Future prospective reactions leading to the neutron-rich transfermium isotopes and having formation cross-sections, that allow collection of appropriate statistics, are listed in the table 2.

Acknowledgements

The project GABRIELA is jointly funded by JINR and IN2P3/CNRS France. Work at FLNR was performed partially under the financial support of the Russian Foundation for Basic Research, Contract No. 08-02-00116 and JINR-BMBF (Germany), JINR-Polish, JINR-Slovak Cooperation Programmes.

References

[1] Z Patyk and A Sobiczewski, *Nucl. Phys.* **A533**, 132 (1991)
[2] S Cwiok *et al*, *Nucl. Phys.* **A611**, 211 (1996)
[3] M Bender *et al*, *Phys. Rev.* **C60**, 034304 (1999)
[4] A T Kruppa *et al*, *Phys. Rev.* **C61**, 034313 (2000)
[5] P Reiter *et al*, *Phys. Rev. Lett.* **82**, 509 (1999)
[6] M Leino *et al*, *Eur. Phys. J.* **A6**, 63 (1999)
[7] P A Butler *et al*, *Phys. Rev. Lett.* **89**, 202501 (2002)
[8] R D Humphreys *et al*, *Phys. Rev.* **C69** 064324 (2004)
[9] P Reiter *et al*, *Phys. Rev. Lett.* **95** 032501 (2005)
[10] R-D Herzberg *et al*, *Phys. Rev.* **C65**, 014303 (2001)
[11] J E Bastin *et al*, *Phys. Rev.* **C73**, 024308 (2006)
[12] A Chatillon *et al*, *International Symposium on Exotic Nuclei, "EXON 2004"*, Peterhof, Russia, July 5–12, 2004 (World Scientific, 2005) p. 198
[13] R-D Herzberg, *J. Phys.* **G30**, R123 (2004)
[14] F P Hessberger *et al*, *Eur. Phys. J.* **A22**, 417 (2004)
[15] F P Hessberger *et al*, *Nucl. Instrum. Methods* **B204**, 597 (2003)
[16] A Chatillon *et al*, *Eur. Phys. J.* **A30**, 397 (2006)
[17] F P Hessberger *et al*, *Eur. Phys. J.* **A12**, 57 (2001)
[18] M Asai *et al*, *Phys. Rev. Lett.* **95**, 102502 (2005)
[19] A G Popeko *et al*, *Phys. At. Nucl.* **69**, 1183 (2006)
[20] K Hauschild *et al*, *Nucl. Instrum. Methods* **A560**, 388 (2006)
[21] O N Malyshev *et al*, *Nucl. Instrum. Methods* **A440**, 86 (2000)
[22] O N Malyshev *et al*, *Nucl. Instrum. Methods* **A516**, 529 (2004)
[23] K Hauschild, *International Symposium on Exotic Nuclei, "EXON 2009"*, Sochi, Russia, September 27–October 3, 2009 (World Scientific, 2010)
[24] K Hauschild *et al*, *Phys. Rev.* **C78**, 021302(R) (2008)
[25] K Hauschild *et al*, *Phys. Rev.* **C77**, 047305 (2008)
[26] A Lopez-Martens *et al*, *Phys. Rev.*, **C74**, 044303 (2006)
[27] A Lopez-Martens *et al*, *Eur. Phys. J.* **A32**, 245 (2007)
[28] C E Bemis, *et al*, ORNL Annual Report (1974) 39
[29] B Streicher, *Synthesis and spectroscopic properties of transfermium isotopes with* $Z =$ 106, 106, 107, Ph.D. thesis (Comenius University, Bratislava, Slovakia, 2006)
[30] H Bartsch *et al*, *Nucl. Instrum. Methods* **121**, 185 (1974)
[31] K H Schmidt, *Eur. Phys. J.* **A8**, 141 (2000)
[32] P F Dittner *et al*, *Phys. Rev. Lett.* **26**, 1037 (1971)